CFD modeling of contaminant capture with an air flow control valve in a full-scale kitchen: an experimental and numerical study

Yusuf OZBAKIS *, Fehmi ERZINCANLI

Department of Mechanical Engineering, Faculty of Engineering, Duzce University, Duzce, Turkey

Abstract

Several studies have utilized commercial CFD software to predict and optimize hood performance in reducing odors. In this study, our objective is to simulate the European standard test using CFD software. To achieve this objective, we modeled a full-scale kitchen and hood-mounted AFCV using Ansys Fluent software. We investigated the impact of hood flow rate and AFCV design on capture efficiency and methyl ethyl ketone (MEK) extraction in detail. The analyzes simulate the capture of the heated water vapor and MEK mixture by the AFCV. The analyzes have been validated with experimental results for different flow rate conditions and have been used with confidence to model the MEK diffusion in a realistic kitchen. Thanks to the innovative AFCV created, an 8% improvement has been achieved in capture performance at a flow rate of 100 m^3/h. The experiments have been repeated at different flow rates, when evaluated in terms of system pressure required for flow rate and energy consumption, approximately 27% savings were achieved at 400m^3/h flow. It is great to hear that this study has provided valuable insights for developing high-efficiency ventilation systems (hood) with improved indoor air quality and low energy consumption for central ventilation systems.

Keywords:

Central ventilation system, Air flow control valve, Energy efficiency, Capture efficiency, Range hood, MEK extraction.

Nomenclature

CFD	Computational Fluid Dynamics
MEK	Methyl Ethyl Ketone
CO	Carbon Monoxide
CO_2	Carbon Dioxide
3D	Three-Dimensional
AFCV	Air Flow Control Valve

Corresponding author: Tel:

E-mail address: yusufozbakis@hotmail.com

Corresponding author present address:

R&D Center, BSH Home Appliances Industry and Trade Inc., Tekirdag, Turkey

1. INTRODUCTION

Human beings need to meet all their needs throughout their life. In particular, they need to eat, sleep and a safe environment to survive [1]. Most food can be prepared by cooking. In kitchens, unwanted smoke and odors are emitted during cooking. Unwanted gases emitted into the environment penetrate the environment when they are not caught and discharged to the outside environment. These gases can spread to other rooms in residences. This undesirable situation negatively affects user comfort [2, 3]. Studies have shown that women and children are exposed to physical ailments such as respiratory tract, eye irritation, headache and low back pain from breathing the fumes caused by cooking food [4, 5].

Recently, numerical and experimental studies have been carried out to thoroughly understand contaminant capture systems found in kitchens and to improve capture efficiency. Singer et al. [6] experimentally tested 15 different home kitchen hoods for design and performance. In the study, the authors observed that pollutant capture performance correlated with hood design, installation configuration (height and angle) and flow rate. OH et al. [7] examined the effect of the gas guide device attached to the hood on the capture performance and emphasized that the capture efficiency is related to the geometry and design. The separator plate added to the kitchen hood had an improvement of 1.4-1.9% in the temperature distribution in the kitchen and 9.4-11.9% in CO_2 emission [8]. In another study, thanks to the innovative valve design, the air flow and the capture speed have been increased and the turbulence density have been reduced [9]. Chen et al. [10] investigated the effects of valve design used in local ventilation systems on capture velocity and turbulence density. In another study, flow in the kitchen was investigated utilizing particle image velocimetry [11]. Logachev et al. [12, 13] conducted research on separated flow in exhaust hoods using both experimental and CFD methods. As stated in study [14], the drag force that causes pressure loss can be reduced by shaping the inlet edges of the hood. Pinelli and Suman [15] investigated the effect of hood size on capture velocity in their study. Huang et al. [16] conducted research on smoke, dust, droplet and waste heat control in industrial ventilation systems. As a result of the study, they have shown that the hood volume is effective in the capture velocity. Wu and Liou [17] conducted a numerical study to investigate how different designs of hood bottom covers can improve the capture efficiency of carbon monoxide (CO). In addition to the existing hood in the study, O, S and V shaped hood bottom cover designs were made. Compared to the existing hood, an improvement of 155.6%, 156.9% and 159.4% was achieved in flow rates, respectively. In another study, the author made a numerical study to prevent smoke and heat dispersion in the kitchen. By adding reverse flow air curtains to the existing hood, the distribution of steam-air mixtures in the kitchen has been examined. As a result, with the reverse air flow added to the hood, the steam-air mixture emitted from the furnace was kept within the hood volume [18]. Hocine et al. [19] investigated in detail the effect of hood flow and fan rotation speed on capture efficiency, CO_2 distribution and velocity profiles. It has been shown that at 100 cfm flow rate, only 65% of the CO_2 dispersion released into the environment is captured. In another study, numerical simulations were performed to model CO_2 extraction with a kitchen hood for different burner configurations. It has been observed that the capture efficiency decreases when the number of burners is increased [20]. The air velocity and CO_2 distribution in the OR was simulated with the CFD method. Kang et al. [21] analyzed the effect of cooking in 30 residential buildings on air quality. As a result of the analysis, it has been shown that the type of cooking is

effective on indoor air quality. Yi et al. [22] conducted a numerical and experimental study to investigate the effect of hood flow rate on hood heat and gas capture efficiency. In the study, experiments were carried out with flow rates between 100 cfm and 350 cfm. Both the heat and gas capture efficiency increased as the flow rate of the hood increased. Liu et al. [23] aimed to investigate the effects of the design features of the air curtain created in the hood flow area on the capture performance. Analyzes were carried out with different jet velocity, jet angle and jet slot width values on the air jet placed in the hood. Oil smoke emission from the pot at 310 ° C and 0.01 kg/s flow rate is defined as the ambient condition. As a result of the study, optimum jet design parameters were determined to improve the kitchen environment. Zhou et al. [24] conducted a field experimental study on push-pull kitchen ventilation system. The results showed that the push-pull ventilation system has effect on the capture performance of the hood. Huang et al. [25] investigated the effects of human body and walking motion on flow characteristics of both wall-mounted and jet-isolated hoods. As a result of the study, it was observed that a cook standing in front of the counter sucked oil fumes and created large turbulent flows, causing a large amount of oil smoke to be dispersed in the kitchen.

There are numerous effective solutions available in international standards for improving ventilation system performance. The primary objective should be to produce better products that meet the needs of people. Central ventilation systems have the ability to draw air from multiple sources simultaneously. These systems utilize AFCVs to regulate the amount of airflow in a specific region. The AFCVs are integrated into the system and can be adjusted to control the flow of air. Additionally, when necessary, the flow of air can be halted completely by closing the valve.

The aim of this study is to simulate the European norm [26] test for central ventilation system hoods using Computational Fluid Dynamics (CFD) software. To achieve this, a full-scale kitchen and an airflow control valve mounted on the hood will be modeled. The analysis focused on simulating the capture of heated water vapor and methyl ethyl ketone (MEK) mixture by the airflow control valve. The model was used with confidence to predict the distribution of MEK in a realistic residential kitchen. The study involved repeating existing and innovative AFCV analyses for four different flow rate scenarios. Time-dependent analyses were validated through experimental tests.

2. Material and Methods

Central ventilation system hoods are subjected to the European norm [26] test. The odor performance of the hood is declared as a result of this test. The aim of this study is to simulate the test in accordance with the European norm with the ANSYS Fluent program. To achieve this, numerical and experimental odor performance tests were conducted on both the existing and newly developed valves. The experimental test results were compared to the numerical analysis results. A detailed schematic of the testing apparatus, along with the materials and methods employed, is depicted in Figure 1.

2.1 Experimental Details

The odor performance test procedure for central ventilation system hoods is specified in the European norm [26]. Figure 2 shows the general dimensions and definitions of the test chamber [26].

Figure 3 shows the testing apparatus and Table 1 shows the devices used in the experiment. Experimental tests were performed in accordance with the procedures specified in the European norm [26].

Based on experimental test data obtained from more than one point in the kitchen, the odor performance (efficiency) calculation was made as in Equation 1 in accordance with the European norm [26].

$$Efficiency = \frac{C_1 - C_2}{C_1} x100 \quad (1)$$

Equivalent: C_1 (ppm) the concentration of MEK in the test chamber before the hood starts working; C_2 (ppm) refers to the MEK concentration at the end of the application when the hood AFCV is open [26].

2.2. Numerical Modeling

CFD software of ANSYS is used for the design and optimization of the devices used in ventilation systems. This saves both time and energy [15]. Thanks to ANSYS software, various formats and values can be selected to calculate the optimum combination of velocity, stability and precision in a given area. In addition, the software can effectively solve problems related to computing complex flows in various fields [17]. In this article, ANSYS Fluent software was used to simulate real environment experiments. Time-dependent analyzes simulating 10 minutes were carried out thanks to the software.

2.2.1. Geometrical modeling

In accordance with European norms [26], wall-mounted hood designs in a 3D full-scale kitchen were performed with the design program Solidworks v20 software. Similarly, a full-scale kitchen was used in another study [27]. General dimensions of the designed 3D model are shown in Figure 4. Kitchen sizes as specified in European norms; length: L = 2500mm, width: W = 3500mm and height: H = 2500mm. The air intake to the kitchen is made through the 700x350mm sized window at the front.

The dimensions of the hood used in the design; length: l = 480mm, width w = 600mm and height: h = 80mm. Since the hood is a central ventilation system hood, it does not contain a fan. Instead, a fully closable air flow control valve (AFCV) is used in the hood. The 3D design of the hood and AFCV used in the experiments is shown in Figure 5. Since the hood exhaust diameter is 150mm, the air flow control valve diameter is designed as 140mm. For comparison, AFCV with a conical structure and 8 air slots, developed as an alternative to the existing AFCV, has been used. The distance between the hood and the cooker is 600mm. The hood is connected to a 150mm diameter and 1000mm long outlet pipe. In order to define the outlet pressure and converge the calculation, a pressure measurement point was created at a distance of 900mm from the hood.

2.2.2. Numerical method

As stated in study [28], local drag values can be determined for fittings adequately using the SST model and the k-ω model. In the field of numerical analysis of ventilation system hoods, certain authors [19, 23, 29] have achieved satisfactory results when using the *k–ω* turbulence model in comparison to experimental data.

In the analyses being referred to, the ANSYS CFD program was used which allows the utilizes the finite volume method to predict fluid flow, and solves the three-dimensional (3D) Reynolds-mean Navier-Stokes equations. A mixture of MEK + water vapor was used to simulate the transport and diffusion of species in the gas simulation from the cooking process. Chemical reactions were ignored in the calculations. Both food smoke concentrations and air movement in the kitchen were taken into account. Simulations are considered as fixed and incompressible. Standard $k - \omega$ turbulence model transport equations, energy conservation equation and conservation equation of species, which do not describe the motion of fluids for multiphase flow, are given below.

Transport equations for the standard $k - \omega$ turbulence model:

$$\frac{\partial}{\partial t}(\rho k) + \frac{\partial}{\partial x_i}(\rho k u_i) = \frac{\partial}{\partial x_j}(\Gamma_k \frac{\partial k}{\partial x_j}) + G_k - Y_k + S_k \quad (2)$$

and

$$\frac{\partial}{\partial t}(\rho \omega) + \frac{\partial}{\partial x_i}(\rho \omega u_i) = \frac{\partial}{\partial x_j}(\Gamma_\omega \frac{\partial \omega}{\partial x_j}) + G_\omega - Y_\omega + S_\omega \quad (3)$$

where k is represents turbulent kinetic energy, ω, the specific dispersion ratio, G_k represents the generation of turbulent kinetic energy due to mean velocity gradients. G_ω represents the generation of ω. S_k and S_ω are user-defined source terms.

Energy conservation equation:

$$\frac{\partial}{\partial t}(\rho h) + \nabla(\rho h \vec{v}) = -\nabla.[(k + k_t)\nabla T] + S_h \quad (4)$$

where k is the molecular conductivity; k_t is the conductivity due to turbulent transport ($k_t = Cp^{\mu}t \,/\, Pr_t$), and term S_h includes defined volumetric heat sources.

Species Transport Equations:

$$\frac{\partial}{\partial t}(\rho Y_i) + \nabla.(\rho \vec{v} Y_i) = -\nabla.\vec{J}_i + S_i \quad (5)$$

where Y_i is the local mass fraction of each species; S_i is the generation rate by addition from user-defined sources. In turbulent flows, the term $\vec{J}_i$ is given by:

$$\vec{J}_i = -(\rho D_{i,m} + \frac{\mu_t}{Sc_t})\nabla.Y_i \quad (6)$$

where S_{C_t} is the turbulent Schmidt number with the expression $S_{C_t} = \mu_t/(\rho D_t)$. μ_t is the turbulent viscosity with the expression $\mu_t = 0.03874\rho vL$, where v is the local velocity magnitude; ρ is the fluid density; L is defined as the distance from the nearest wall, and 0.03874 is an empirical constant [30].

The finite volume method is a numerical technique for approximating solutions to partial differential equations by dividing the domain into a set of finite volumes or cells, and then discretizing the differential equations on a per-volume basis.

The use of the second-order upwind scheme for differential derivatives and the coupled scheme for pressure-dependent equations are common numerical techniques used in the finite volume method to improve accuracy and stability. The use of time-dependent analysis is also common in the study of fluid dynamics, as it allows for the observation of dynamic changes over time.

The application of the incompressible ideal gas equation to obtain the variation of air density with different temperatures is also a relevant step in the analysis of fluid flow, as it is often necessary to consider the compressibility of gases when studying fluid dynamics.

Therefore, assuming that the context of the statement is appropriate, it can be considered a valid and accurate description of the methodology used to study fluid dynamics using the finite volume method and related numerical techniques.

2.2.3. Boundary conditions and mesh model

To determine the boundary conditions suitable for mathematical modeling, some assumptions have been made on the physical parameters in this article: 1) the only air intake in the kitchen is the ventilation window and the only airflow outlet at the hood exhaust outlet; 2) the air temperature in the kitchen is 23 °C; 3) represents the cooking process, the mixture of MEK + water vapor exiting the pot; 4) the experiment pan is at a temperature of 170 °C; 5) Chef movements in the kitchen were not taken into account in this study.

Figure 6 shows the boundary conditions for the analysis area. In the calculations, the boundary condition was accepted as 1 atm ambient pressure and 23 ° C. The pressure value simulating the hood flow rate is defined in the hood outlet area. For experimental verification tests, a pressure measurement point has been defined 900mm ahead of the hood outlet. The test pot shown in Figure 6 is the heat source and release point for MEK + water vapor. The temperature of the MEK + water vapor leaving the experiment pot was set at 170 °C and its flow rate as 0.0001667 kg/h. All adjustments simulate the test conditions defined in the European norm [26]. Cooking process causes a temperature rise of about 10.0°C around the person sitting in the kitchen [29]. In order to examine the temperature distribution in the room, a plane referencing the center of the test pot was added.

Describes the process of preparing a numerical mesh for analysis using Solidworks and ANSYS modules, along with Fluent Meshing software. In the meshing stage, the geometry is divided into small solution cells using the finite element method. The number of elements is determined based on the expected quality of the solution results, and a polyhedral mesh structure is used for the analysis, which allows the creation of elements of every mesh quality in complex geometries with fewer elements. Local improvements were made to accurately capture the MEK distribution in the region between the test pan and the hood, and 2.8 million mesh elements were used in this region. The total number of mesh elements in the model is 9 million, which refers to the number of small geometric shapes used to approximate the larger geometric shape of the model. The skewness value is a measure of the quality of the mesh model network, which refers to how well the mesh elements are distributed throughout the model. A skewness value between 0 and 1 is used to represent the distribution of the mesh elements, with a value below 0.95 being considered acceptable. The statement indicates that the maximum skewness value in the model was 0.82, which is below the acceptable limit of 0.95, indicating that the mesh model is of good quality. Lv et al. [31] in their study, defined the (y+ <5) value as reasonable in the analyzes to be made for the SST k–ω turbulence model. The mesh model structure created in the study meets the Reynolds number approach requirement (2< (y+) <5).

Sensitivity analysis of approximately 2.2 million, 6 million and 9 million cells was performed for the optimum mesh element number. As a result of the analysis, the maximum discrepancy in the flow rate value is approximately 9%, 3% and 1%, respectively. As a result, the mesh element structure that provides the best convergence on the flow rate value was selected. The mesh structure as a result of the mesh created is shown in Figure 7.

3. VALIDATION TEST CASES

When determining boundary conditions for analyses, the actual ambient conditions should be considered. Otherwise, numerical analysis results will be inconsistent with experimental results. Verification of the numerical analysis created was made by experimental flow measurements. The system pressure values required for the flow rate (100,200,300,400 m^3/h) determined in the study were measured with 2 different models. Each measurement was repeated three times and averaged. Flow rate and required system pressure measurements were made in the accredited testing laboratory with volumetric flow rate and performance test device. System pressures required for 2 different models and 4 different flow rates were used in numerical analysis. In similar studies, the authors [19, 23] obtained satisfactory results compared to the experimental data using the k - ω turbulence model. In the study, the k - ω SST turbulence model was used. System pressures with a turbulence density of 5% in the hood exit area, simulating the flow capacity, are defined. Analyzes were repeated for 2 models and 4 different system pressures. Flow rate-pressure graphs formed as a result of experimental and numerical analysis are given in Figure 8.

When the verification test results were examined, it was observed that there was a maximum deviation of 5.8% in the flow rate values. Therefore, the numerical analysis created in AFCV development analysis can be

used safely. In the analysis made within the scope of the study, the adjustments used in the validation experiments were used.

4. RESULTS and DISCUSSION

4.1. Numerical Analysis Results

Numerical analysis was repeated in 4 different flow rates for each 2 valve models. As a result, the distribution of MEK in the kitchen was examined. In order to measure the ability of the hood to remove MEK released from the experiment pot at different flow rates, the capture efficiency was calculated as in Equation 1 according to the European norm [26]:

The odor capture efficiency values obtained as a result of the analyzes and calculations are given graphically in Figure 9.

In the analysis, a strong correlation was observed between capture efficiency and flow rate. Increasing the flow rate from 100 m^3/h to 300 m^3/h resulted in a linear increase in capture efficiency, similar to other studies [19, 22]. Increasing the flow rate from 100 m^3/h to 300 m^3/h increased the capture efficiency by approximately 30%. When the flow rate reaches a certain value above 300 m^3/h, the capture efficiency remained insensitive to the flow rate change and reached 100%. In the analyzes, the effect of AFCV design on odor capture performance was investigated. Figure 10 shows the distribution of MEK in the kitchen after 10s at 100 m^3/h flow. When the MEK distribution is examined, it is seen that new model has a superior performance.

For examine the distribution of MEK in the kitchen in accordance with the European norm [26]; The analyzes were made depending on the time and to simulate the 10-minute period.

Figure 11 shows the MEK distribution at a flow rate of 100 m^3/h for different model AFCVs in the front view of the kitchen. MEK released from the pot has been spread into the kitchen as it could not be caught by the hood at a flow rate of 100 m^3/h. This distribution is related to the capture efficiency value shown in Figure 11 where only 57% (Current model) and 62% (New model) of the MEK released from the pot were caught. The values calculated in the study are similar to the other studies [19, 20].

The distribution of MEK in the kitchen has gradually disappeared with the increase of flow rate. It has been observed that as the flow rate increases, the MEK released from the pot is directed towards the hood. Figure 12, in the front and side view of the kitchen, it is clearly seen that at a flow rate of 200 m^3/h, the MEK hood escapes from the front and left edge areas and disperses into the kitchen. It is seen that the MEK released from the pot at 300 m^3/h flow rate (Figure 13) escapes from the left and front edges of the hood and disperses into the kitchen in Current model. In New model, the MEK escaping from the hood is too small to be seen. This result is an indication of the increase in catching performance with the innovative valve developed. It was observed that

the MEK emission was caught by the hood in both models at a flow rate of 400 m^3/h. These results are similar to other studies [19].

4.2. Experimental Result

4.2.1. Odour Test Results

In this study, it is aimed to use numerical analysis instead of experimental tests in the development of AFCV. The distribution of MEK in the kitchen has been calculated under real environment conditions with the help of numerical analysis. In order to verify the analysis, experimental measurements (Table 2) were made at 4 different flow rates of 2 different valve models. For the experiments, 2 different AFCV-connected hood prototypes (Figure 14) were created. Hoods were connected to the scent room, respectively, and the system pressure was adjusted by the central system fan for the flow rate determined in the experiment. Odor capture performance measurements were made in the accordance laboratory with the international norm [26] as shown in Figure 3. An air disturbance simulating the movements of the cook was used in the experiments. Disturbance was moved back and forth over a distance of 2 m at 0.5 m/s per hour throughout the experiment. After the tests, the MEK concentration was measured from the points in the odor chamber and the odor capture performance was calculated (Equation 1). Experiments were repeated three times and average values were taken in calculations. The values obtained as a result of the tests are given in Table 2.

As a result of the experiments, while 52.7% odor performance was achieved with Current model at 100 m^3/h flow rate, 57.1% odor performance was achieved with improved AFCV (New model). Thanks to the improved AFCV, an improvement of approximately 8% in odor performance has been achieved at a flow rate of 100 m^3/h. Compared to the increase in the flow rate, there was an increase in the odor capture performance in both models. In addition, thanks to the innovative valve, while increasing the odor performance at the same flow rate, the necessary system pressure has been saved. When evaluated in terms of the system pressure required for the same flow rate, approximately 25% of the system pressure has been saved in all flow conditions. The determined results will guide further studies.

Figure 15 shows the experimental and numerical results calculated for both models with different flow rates. When the experimental and numerical analysis results were compared, the maximum deviation was 8%. Similarly, Xing et al. [32] obtained a maximum discrepancy of 8% between numerical and experimental results in their study on CO_2 transport and diffusion. The low odor performance in the experimental study and the fact that the odor performance reached 100% in numerical analysis is due to the ignoring of the cook movements in the kitchen in numerical analysis. In the experimental tests, an air diffuser (Figure 2) simulating the cook was used.

4.2.2. Energy Consumption Test Results

For energy consumption measurement, a power measuring device is connected to the central system fan of the odor performance measurement room (Figure 3). With the help of the central system fan control panel, the flow rate was adjusted and the energy consumption of the central system fan was measured. Energy consumption

measurements were repeated 3 times and average values were taken. Figure 16 shows, the energy consumption of the central system fan measured for both models at different flow rates. When the energy consumption values of the current AFCV and the AFCV developed with a conical structure are compared 10% at 100 m^3/h flow, 17% at 200 m^3/h flow, 22% at 300 m^3/h flow and 27% at 400 m^3/h flow energy savings have been achieved.

With the increase in flow, the energy consumption values increased in both models. In the current model, the increase in energy consumption was 145%, 140% and 112%, respectively, compared to the 100% flow rate increase. In the new model, the increase in energy consumption was 126%, 126% and 96%, respectively, compared to the 100% flow rate increase. The newly developed AFCV model resulted in a lower increase in energy consumption compared to the current model when the system flow rate increased.

5. CONCLUSIONS

This study analyzed the MEK capture dynamics in a full-scale kitchen using Ansys Fluent software, and compared the numerical results with experimental findings. The research explored the impact of hood flow rate and AFCV design on capture efficiency, MEK dispersion, and energy consumption in detail.

To verify the numerical analysis, the results from both the numerical and experimental analyses were compared. The verification experiments showed a maximum deviation of 5.8% in the flow rate results at the same ambient conditions. Since the experimental and numerical analysis results were found to be compatible, the numerical method created can be considered reliable for use.

The numerical method used in this study has been guided the development of an innovative AFCV. Commercial businesses can save time and energy by avoiding multiple prototyping and experimental tests using this numerical method in odor analysis.

Compared to the existing AFCV (Current model), the innovative AFCV (New model) demonstrated an increase in catch performance in the kitchen, resulting in a reduction in MEK dispersion and temperature distribution. The use of the innovative valve led to a saving of approximately 25% in the required system pressure for the entire flow condition. Additionally, energy consumption values were found to be 10% to 27% lower under different conditions.

When evaluated in terms of the increase in flow in the system, the energy consumption of the central system fan increased with the increase in flow rate. However, the extent of this increase varied based on the AFCV design.

This study provides valuable insights into the development of high-efficiency ventilation systems with improved indoor air quality and low energy consumption for central ventilation systems. Future studies could investigate the effects on odor performance by simulating the movements of the cook.

ACKNOWLEDGMENT

It indicates that the study in question received financial support from TUBITAK, a research council in Turkey, and provides the project number(3190623) associated with the funding. It expresses gratitude towards Silverline Industry and the personnel of the R&D department for their assistance in this project.

REFERENCES

1. Maslow, A.H., Motivation and Personality, Harper & Brothers, New York (1954).
2. Wang, P., Liu, S., Liu, J., et al., "Size-resolved splashed cooking oil droplets from 1 to 1000 μm on surfaces: The impact of residential range hoods", Building and Environment, **210**, 108705 (2022).
3. Anderson, J.O., Thundiyil, J.G. and Stolbach, A., "Clearing the air: a review of the effects of particulate matter air pollution on human health", Journal of Medical Toxicology, **8** (2), pp. 166-175 (2012).
4. Dherani, M., Pope, D., Mascarenhas, M., et al., "Indoor air pollution from unprocessed solid fuel use and pneumonia risk in children aged under five years: a systematic review and meta-analysis", Bulletin of the World Health Organization, **86**, pp. 390-398 (2008).
5. Tielsch, J.M., Katz, J., Thulasiraj, R.D., et al., "Exposure to indoor biomass fuel and tobacco smoke and risk of adverse reproductive outcomes, mortality, respiratory morbidity and growth among newborn infants in south India", International journal of epidemiology, **38** (5), pp. 1351-1363 (2009).
6. Singer, B.C., Delp, W.W., Price, P., et al., "Performance of installed cooking exhaust devices", Indoor Air, **22** (3), pp. 224-234 (2012).
7. Oh, Y.K., Kim, Y.S., Yoon, H.S.,"A study on improvement capture velocity for increasing inhalation efficiency of hood in local ventilation system", Advanced Materials Research (2008). Trans Tech Publ.
8. Lim, K. and Lee, C., "A numerical study on the characteristics of flow field, temperature and concentration distribution according to changing the shape of separation plate of kitchen hood system", Energy and Buildings, **40** (2), pp. 175-184 (2008).
9. Ozbakis, Y. and Erzincanli F., "Air flow control valve development with reinforced operating parameters", Surface Review and Letters, **28** (12) (2021).
10. Chen, W., Liu, J., Mak, C.M., et al., "Near fields of annular slotted hoods measured via 2D-PIV", Building and Environment, **144**, pp. 1-8 (2018).
11. Chen, W., Liu, J., Li, J., Dai, X., et al., "Assessment of a confined thermal plume by PIV combined with POD analysis", Applied Thermal Engineering, **188**, 116590 (2021).
12. Logachev, K., Ziganshin, A., Averkova, O., et al., "A survey of separated airflow patterns at inlet of circular exhaust hoods", Energy and Buildings, **173**, pp. 58-70 (2018).
13. Logachev, K. I., Ziganshin, A. M., Huang, Y., et al., "Developing a mathematical simulation method for three-dimensional separated airflow at inlet of local exhaust devices", Journal of Building Engineering, **63**, 105490, (2023).
14. Logachev, K. I., Ziganshin, A. M., Popov, E. N., et al., "Experiment determining pressure loss reduction using a shaped round exhaust hood", Building and Environment, **190**, 107572, (2021).
15. Pinelli, M. and Suman, A., "A numerical method for the efficient design of free opening hoods in industrial and domestic applications", Energy, **74**, pp. 484-493 (2014).
16. Huang, Y., Wang, Y., Ren, X., et al., "Ventilation guidelines for controlling smoke, dust, droplets and waste heat: Four representative case studies in Chinese industrial buildings", Energy and Buildings, **128**, pp. 834-844 (2016).
17. Wu, W.-C. and Liou, J.-Y., "Numerical simulation of harmful gas distribution in a range hood with an improved flow channel", Microelectronics Reliability, **99**, pp. 245-261 (2019).
18. Kecel, S., "Preventing Odor Diffusion: An Innovative Hood Design", Gazi University Journal of Science, **30** (4), pp. 1-13 (2017).
19. Le Hocine, A.E.B., Poncet, S. and Fellouah, H., "CFD modeling of the CO2 capture by range hood in a full-scale kitchen", Building and Environment, **183**, 107168 (2020).
20. Le Hocine, A.E.B., Poncet, S. and Fellouah, H., "Numerical simulation of the capture efficiency of a domestic range hood for different burner scenarios", Proceedings of the Canadian Society for Mechanical Engineering International Congress, Charlottetown, Canada, (2020).
21. Kang, K., Kim, H., Kim, D.D., et al., "Characteristics of cooking-generated PM10 and PM2. 5 in residential buildings with different cooking and ventilation types", Science of the total environment, **668**, pp. 56-66 (2019).
22. Yi, K.W., Kim, Y.I. and Bae, G.-N., "Effect of air flow rates on concurrent supply and exhaust kitchen ventilation system", Indoor and Built Environment, **25** (1), pp. 180-190 (2016).

23. Liu, X., Wang, X. and Xi, G., "Orthogonal design on range hood with air curtain and its effects on kitchen environment", Journal of occupational and environmental hygiene, **11** (3), pp. 186-199 (2014).
24. Zhou, B., Wei, P., Tan, M., et al., "Capture efficiency and thermal comfort in Chinese residential kitchen with push-pull ventilation system in winter-a field study", Building and Environment, **149**, pp. 182-195, (2019).
25. Huang, R., Lin, S., Jan, S.-Y., et al., Chang, C.-P., Shih, T.-S. and Chen, C.-C., "Aerodynamic characteristics and design guidelines of push–pull ventilation systems", Annals of occupational hygiene, **49** (1), pp. 1-15, (2005).
26. Cooking Fume Extractors – Methods for Measuring Performance. 2019, Standart: IEC International.
27. Luo, M., Guo, J., Feng, X. and Chen, W., "Studying occupant's heat exposure and thermal comfort in the kitchen through full-scale experiments and CFD simulations", Indoor and Built Environment, 1420326X221147161 (2022).
28. Rudenko, N., Babushkin, Y. and Fursova, I., "CFD Technology for Use in Optimizing Fittings for Ductwork", In Proceedings of the XIII International Scientific Conference on Architecture and Construction 2020, pp. 605-612, Springer, Singapore (2021).
29. Liu, Y., Li, C., Ma, H., et al., "Investigation on the indoor environment during a whole cooking process under constant make-up air organization in a Chinese-style residential kitchen", Indoor and Built Environment, 1420326X231152554 (2023).
30. Zhou, B., Chen, F., Dong, Z., et al., "Study on pollution control in residential kitchen based on the push-pull ventilation system", Building and Environment, **107**, pp. 99-112 (2016).
31. Lv, L., Gao, J., Zeng, L., et al., "Performance assessment of air curtain range hood using contaminant removal efficiency: An experimental and numerical study", Building and Environment, **188**, 107456, (2021).
32. Xing, J., Liu, Z., Huang, P., et al., "Experimental and numerical study of the dispersion of carbon dioxide plume", Journal of hazardous materials, **256**, pp. 40-48, (2013).

Figure and Table Captions

List of Figures

Figure 1. Detailed schematic picture of the testing apparatus.

Figure 2. Odour extraction performance test chamber.

Figure 3. Testing apparatus.

Figure 4. 3D dimensions of the test chamber

Figure 5. Extended view of the range hood.

Figure 6. 3D drawing of the computing area.

Figure 7. Different views of the mesh distribution.

Figure 8. Validation test results. System pressure for different flow rates.

Figure 9. Numerical test results. Capture efficiency for different flow rates.

Figure 10. MEK distribution formed in the kitchen after 10s at a flow rate of 100 m^3/h.

Figure 11. MEK distribution in the kitchen at 100 m^3/h flow rate.

Figure 12. MEK distribution in the kitchen at a flow of 200 m^3/h.

Figure 13. MEK distribution in the kitchen at a flow of 300 m^3/h.

Figure 14. Hood prototypes created for experiments.

Figure 15. Capture efficiency for different flow rates.

Figure 16. Energy consumption and system pressure during experiments.

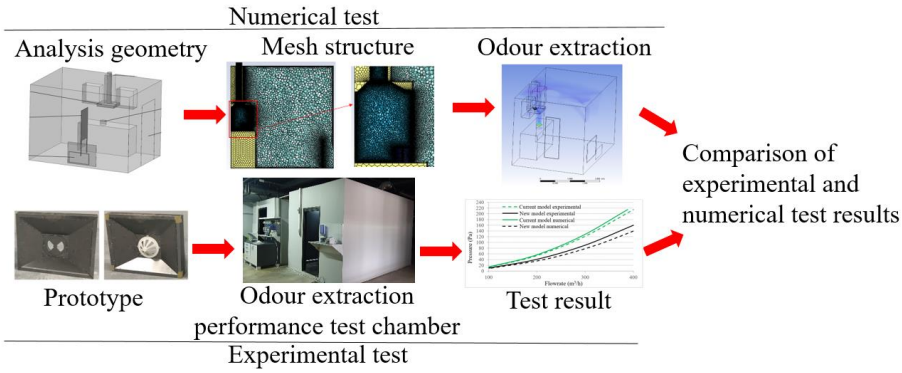

Figure 1. Detailed schematic picture of the testing apparatus.

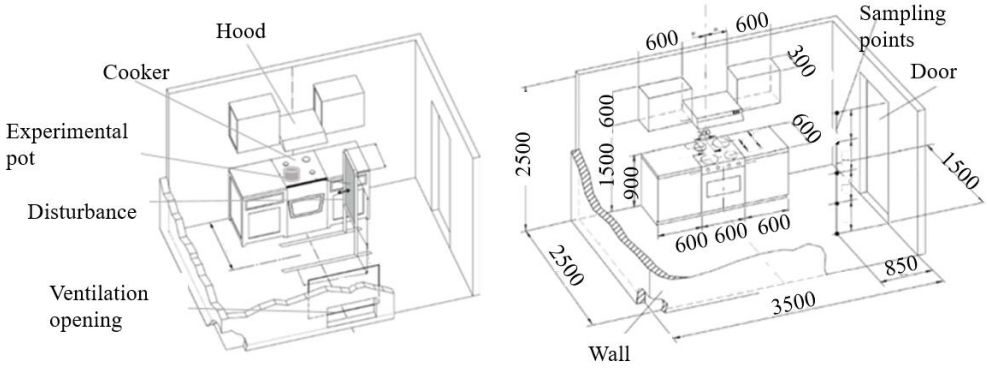

Figure 2. Odour extraction performance test chamber [26].

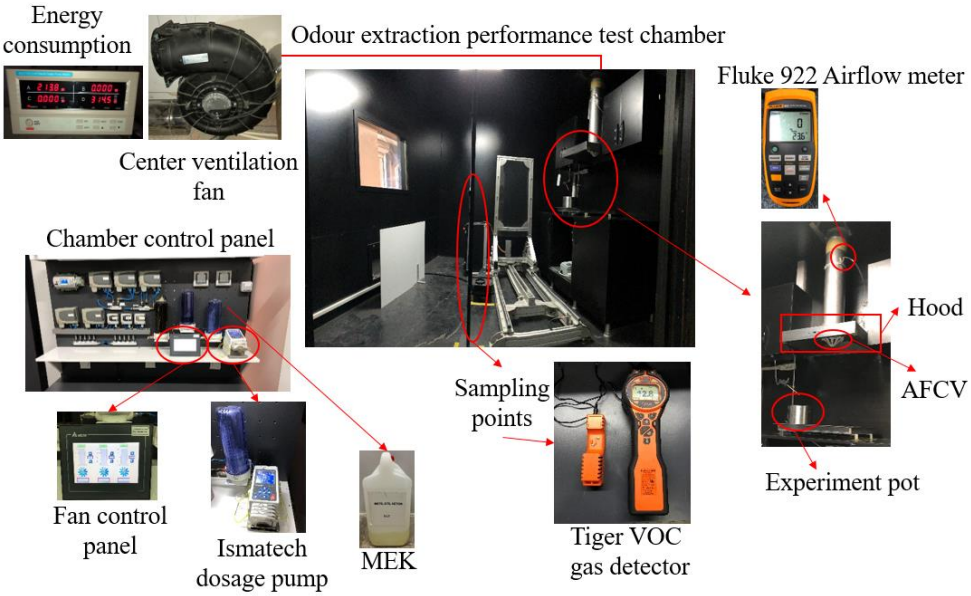

Figure 3. Testing apparatus.

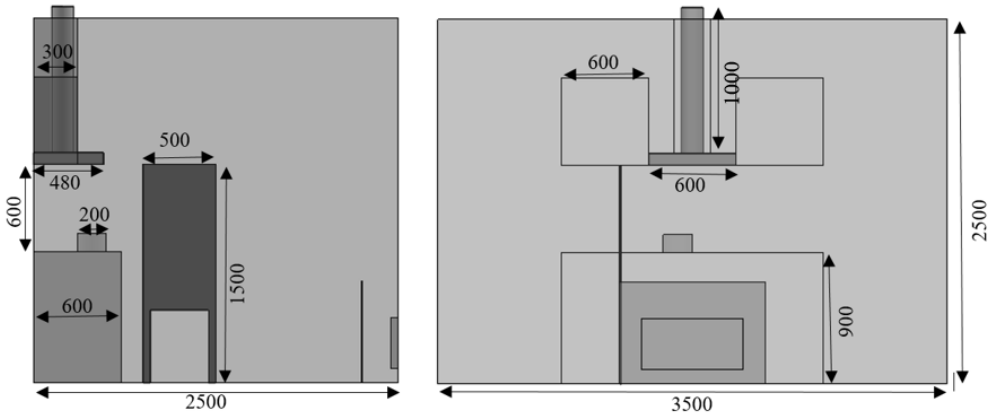

Figure 4. 3D dimensions of the test chamber

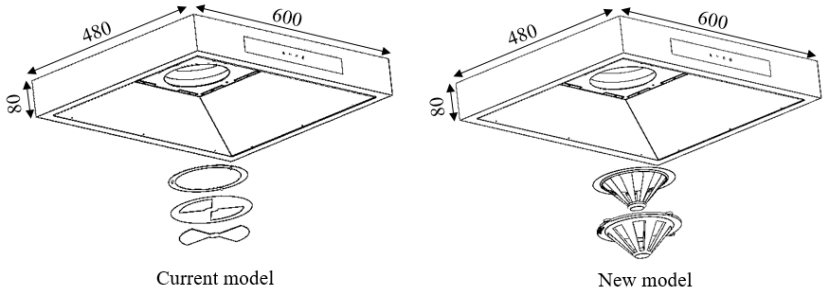

Figure 5. Extended view of the range hood.

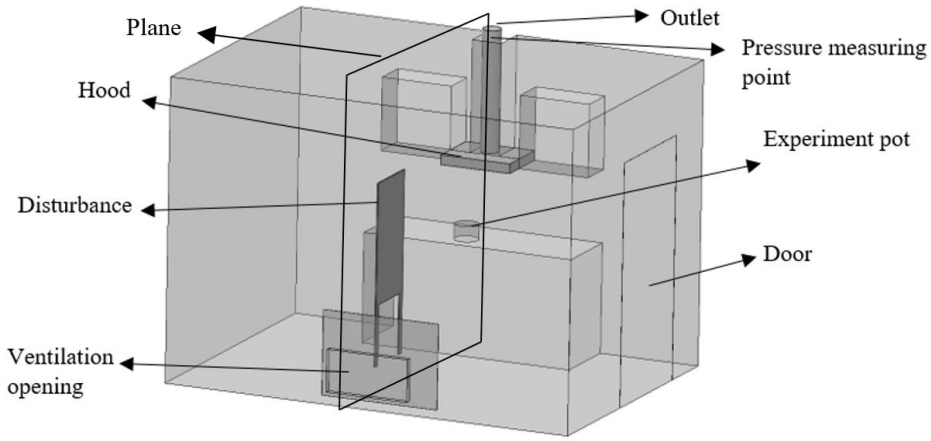

Figure 6. 3D drawing of the computing area.

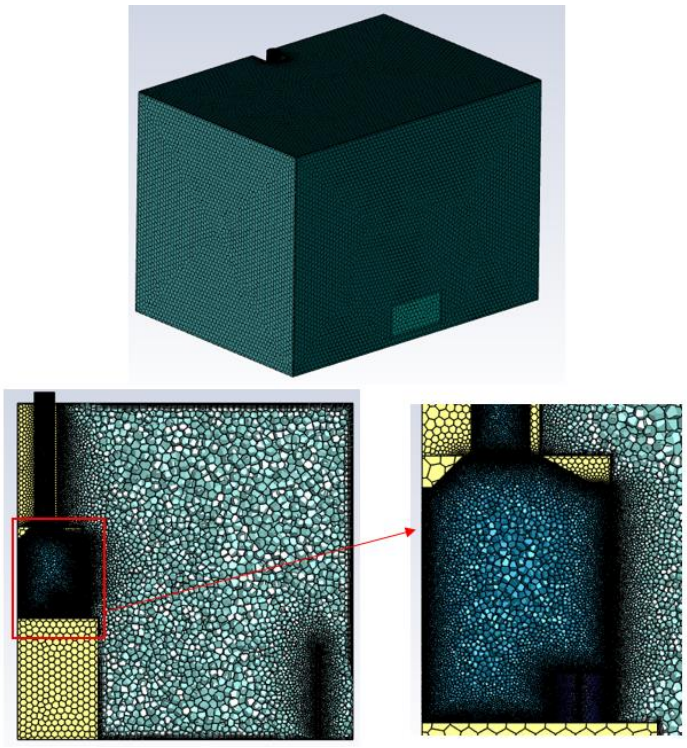

Figure 7. Different views of the mesh distribution.

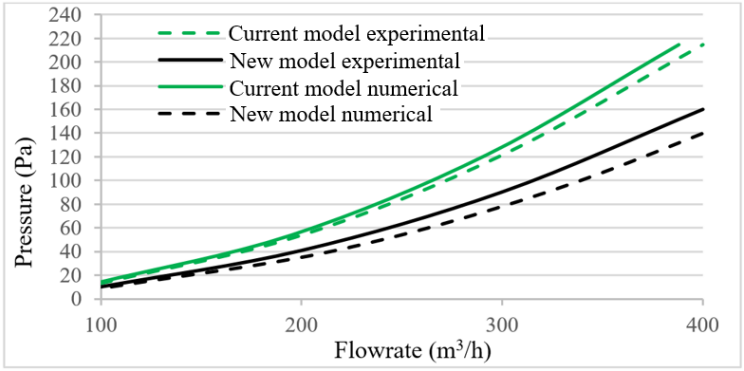

Figure 8. Validation test results. System pressure for different flow rates.

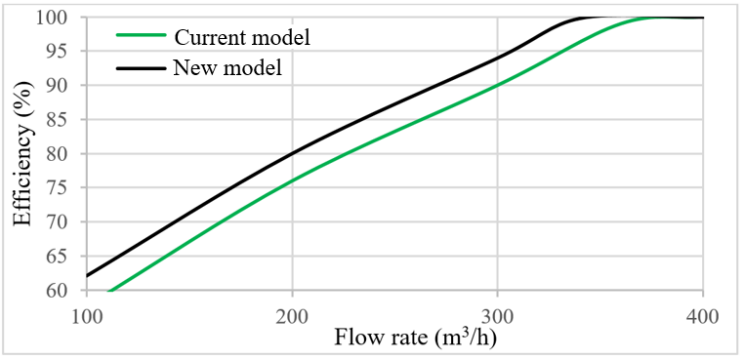

Figure 9. Numerical test results. Capture efficiency for different flow rates.

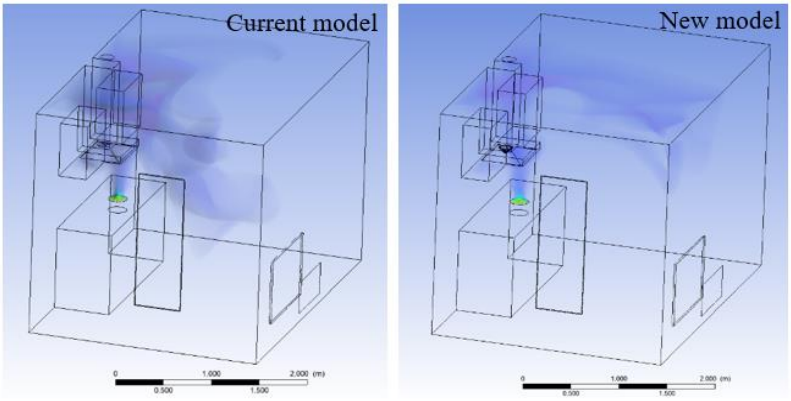

Figure 10. MEK distribution formed in the kitchen after 10s at a flow rate of 100 m^3/h.

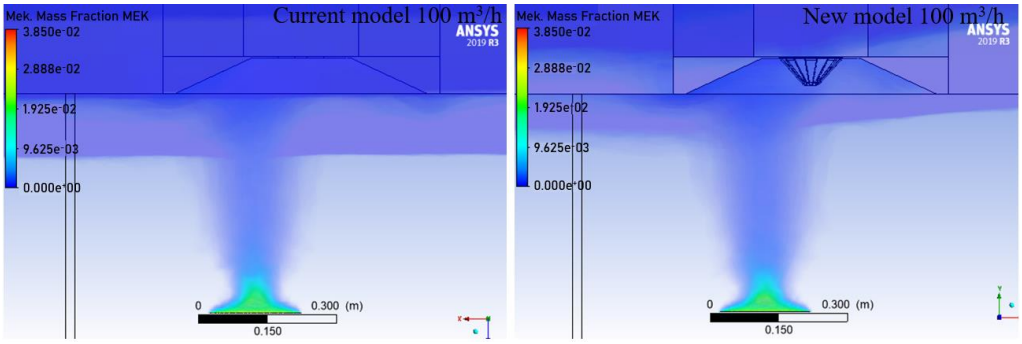

Figure 11. MEK distribution in the kitchen at 100 m^3/h flow rate.

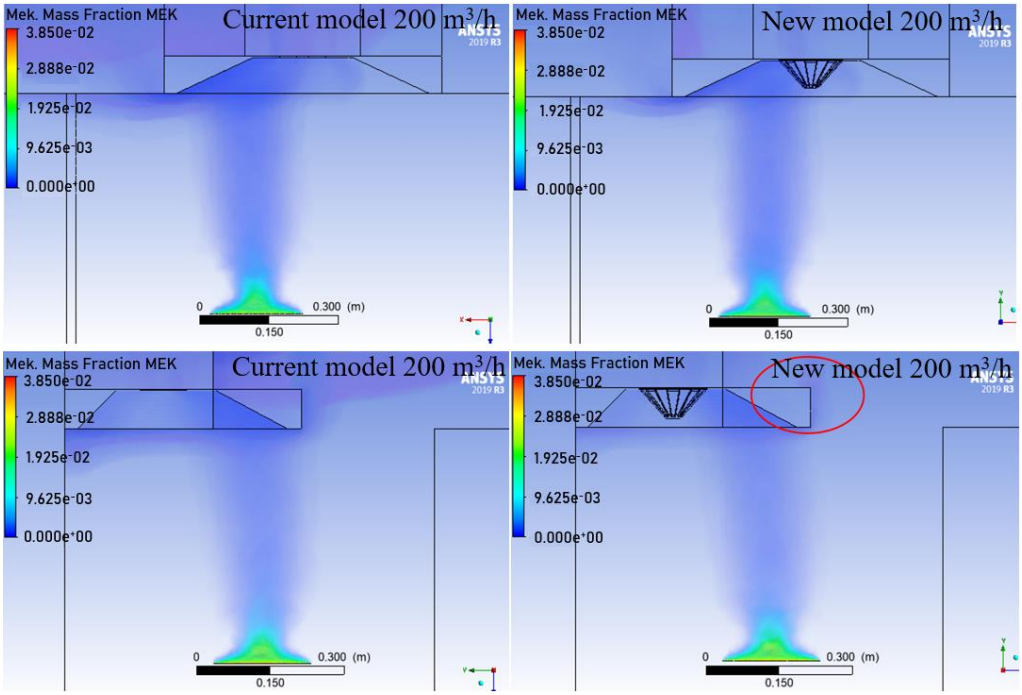

Figure 12. MEK distribution in the kitchen at a flow of 200 m^3/h.

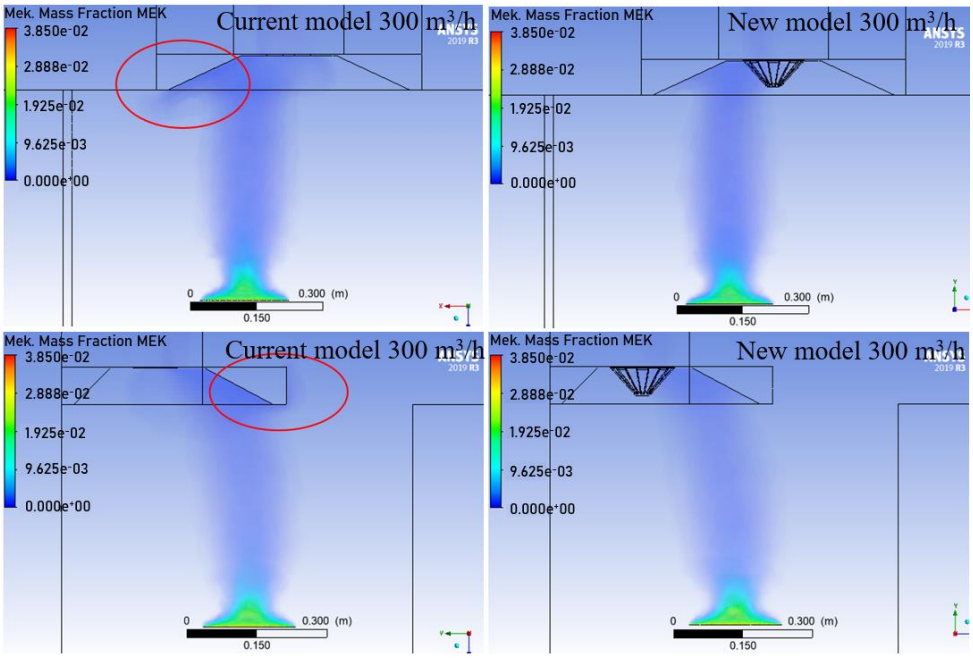

Figure 13. MEK distribution in the kitchen at a flow of 300 m^3/h.

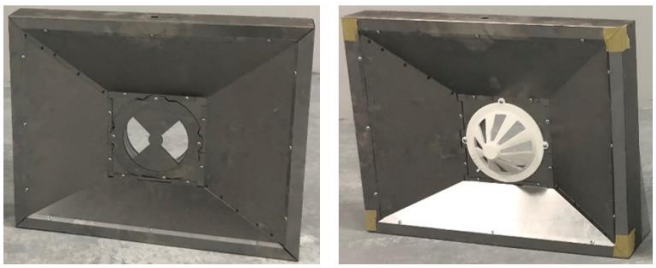

Figure 14. Hood prototypes created for experiments.

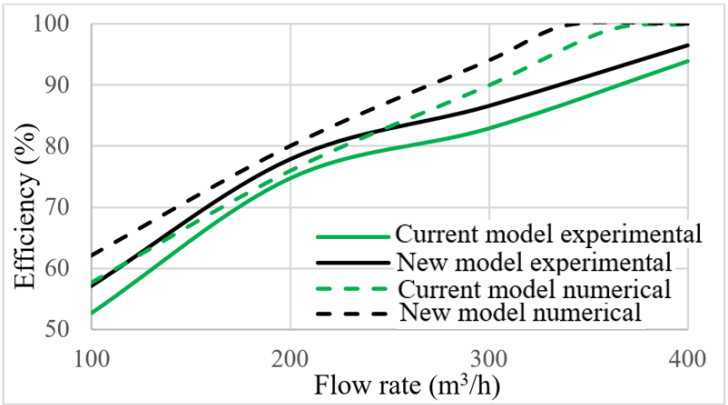

Figure 15. Capture efficiency for different flow rates.

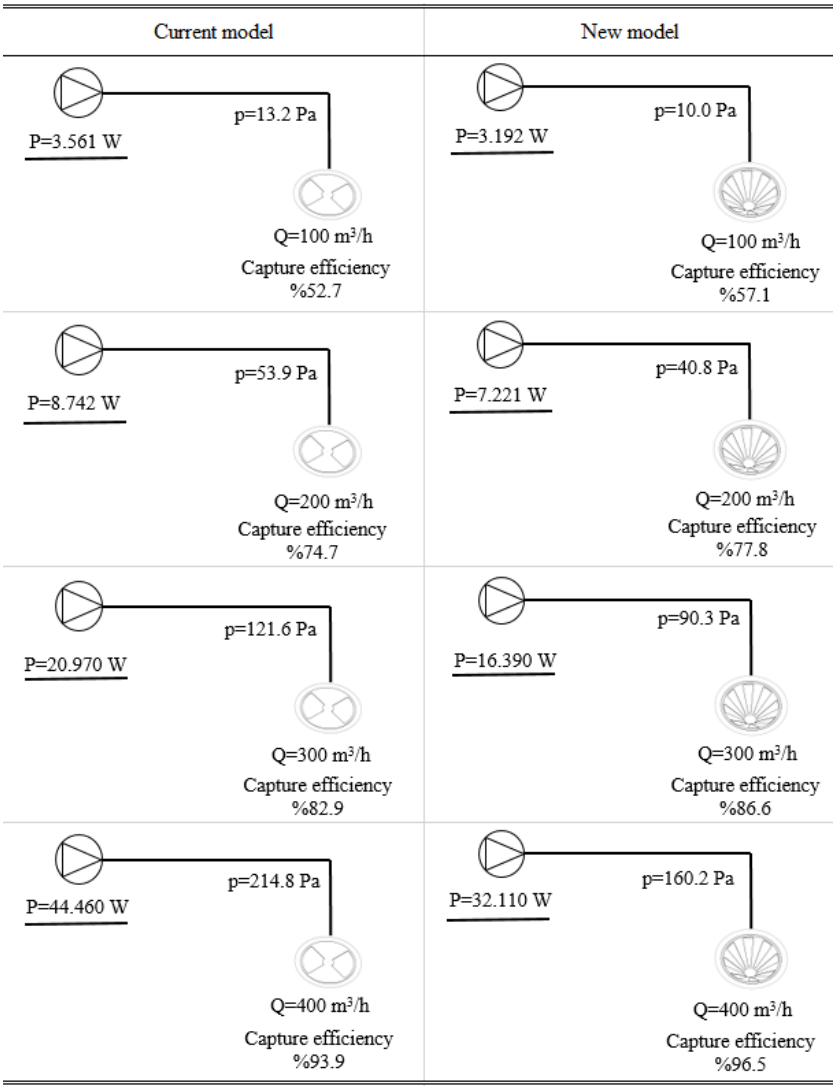

Figure 16. Energy consumption and system pressure during experiments.

List of Tables

Table 1. Descriptive info about the testing instruments.

Table 2. Descriptive information about the experimental instruments.

Table 1. Descriptive info about the testing instruments.

Measuring target	Measuring instrument
Flowrate (m^3/h)	Fan control panel (Delta)
System pressure (Pa)	Airflow meter (Fluke 922)
MEK measurement (ppm)	Gas detector (Tiger VOC)
MEK dosing	Dosage pump (Ismatech)
Energy consumption (W)	Multitech Digital Power Meter (MT9940N)
Heater	Induction cooker
Fan	Center ventilation fan (ebm-papst G3G225-RE07-03)
Prototype	3D Printing (Stratasys Objet260)

Table 2. Descriptive information about the experimental instruments.

Experiment Number	Model	Valve Position	Pressure (Pa)	Flow rate (m^3/h)	C_1 (ppm)	C_2 (ppm)	Efficiency (%)
1	Current	Full	13.2	100	59.4	28.4	52.7
2	Current	Full	53.9	200	59.4	15.2	74.7
3	Current	Full	121.6	300	59.4	10.3	82.9
4	Current	Full	214.8	400	59.4	3.7	93.9
5	New	Full	10.0	100	59.4	25.8	57.1
6	New	Full	40.8	200	59.4	13.3	77.8
7	New	Full	90.3	300	59.4	8.1	86.6
8	New	Full	160.2	400	59.4	2.1	96.5

Prof. Dr. Fehmi Erzincanli is retired as a Professor from the Department of Mechanical Engineering, Düzce University, Düzce, Türkiye. He is founder of Ertekno company. He has Published more than 50 research papers in international journals and conferences. He advised many master's and doctoral theses. His research interests include CFD analysis, industry 4.0 , manufacturing methods, optimization and reliability

Dr. Yusuf Ozbakis is currently a R&D Executive at the BSH Home Appliances Industry and Trade Inc., R&D Center, Tekirdağ, Türkiye. He has done his PhD from the Department of Mechanical Engineering, Düzce University in 2022. His research interests include CFD analysis, manufacturing methods, aviation industry, optimization and reliability. He has Published 15 research papers in international journals and conferences. He has many patents.